NSL 17964

ELSEVIER

Neuroscience Letters xx (2001) xxx–xxx

Neuroscience Letters

www.elsevier.com/locate/neulet

Two mutations in the IV/S4-S5 segment of the human skeletal muscle Na^+ channel disrupt fast and enhance slow inactivation

Alexi K. Alekov[a], Wolfgang Peter[a], Nenad Mitrovic[a,b], Frank Lehmann-Horn[a], Holger Lerche[a,b,*]

[a]*Department of Applied Physiology, University of Ulm, D-89069 Ulm, Germany*
[b]*Department of Neurology, University of Ulm, D-89069 Ulm, Germany*

Received 11 April 2001; received in revised form 3 May 2001; accepted 3 May 2001

Abstract

Fast and slow inactivation (FI, SI) of the voltage-gated Na^+ channel are two kinetically distinct and structurally dissociated processes. The voltage sensor IV/S4 and the intracellular IV/S4-S5 loop have been shown to play an important role in FI mediating the coupling between activation and inactivation. Two mutations in IV/S4-S5 of the human muscle Na^+ channel, L1482C/A, disrupt FI by inducing a persistent Na^+ current, shifting steady-state inactivation in the depolarizing direction and accelerating its recovery. These effects were more pronounced for L1482A. In contrast, SI of L1482C/A channels was enhanced showing a more complete SI and a 3-fold slowing of its recovery. Effects on SI were more pronounced for L1482C. The results indicate an important role of the IV/S4-S5 loop not only in FI but also in SI of the Na^+ channel.

Keywords: Ion channel; Patch clamp; Myotonia; Paralysis

Voltage-gated Na^+ channels are responsible for the initiation and conduction of action potentials in nerve and muscle cells. Their gating is characterized by a fast activation upon depolarization followed by 'fast inactivation' (FI) within a few milliseconds. 'Slow inactivation' (SI) acts on a time scale of seconds. Whereas FI is required to guarantee a rapid repolarization of the cell membrane after an action potential, the physiological role of SI is not entirely known. However, both processes can be disrupted by mutations causing rare hereditary diseases, such as myotonia, hyperkalemic periodic paralysis, long QT syndrome or a form of epilepsy [1,9].

The Na^+ channel α-subunit contains four domains (I-IV) of six transmembrane segments each (S1-S6). S5-S6 loops form the ion conducting pore, S4 segments the voltage sensor and the III-IV cytoplasmic loop contains the proposed 'inactivation particle' (IFM) for FI which may occlude the channel pore [4]. Several sites on the cytoplasmic surface of the protein, which may directly or indirectly contribute to a receptor for the IFM, affect FI [4,9].

The mechanism of SI is less well understood. Channel parts that have been shown to be involved in SI are the pore [2], the II/S4-S5 loop [5,8], the voltage sensors IV/S4 [1,13] and II/S4 (unpublished results from our group[15]), segments IV/S5 [3] and IV/S6 [8]. FI and SI seem to be rather independent processes. Although SI is accelerated in some mutants lacking FI [6,14], it is not in others [5,8], and the accessibility of the IFM-motif is independent of SI [16].

The IV/S4-S5 intracellular loop and the connected voltage sensor IV/S4 play an important role in FI. Outward movement of IV/S4 should initiate a conformational change of IV/S4-S5 and other regions leading to the formation of a receptor site for the inactivation particle thereby coupling FI to activation [7,10,11,12]. The aim of this study was to evaluate effects on SI of IV/S4-S5 mutations which have not been reported so far.

Site-directed mutagenesis to introduce the mutations L1482A/C has been described elsewhere [10,12]. WT and mutant plasmids were transfected transiently in the mammalian cell line tsA201 [10]. Standard whole-cell recording was performed using an EPC-7 amplifier (List). Pipette solution (in mM): 105 CsF, 35 NaCl, 10 EGTA, 10

* Corresponding author. Departments of Applied Physiology and Neurology, University of Ulm Zentrum Klinische Forschung, Helmholtzstr, 8/1 D-89081 Ulm, Germany. Tel.: +49-731-503-3616/+49-731-177-5212; fax: +49-731-503-3609.

E-mail address: holger.lerche@medizin.uni-ulm.de (H. Lerche).

0304-3940/01/$ - see front matter
PII: S0304-3940(01)01895-X

Hepes, (pH 7.4). Bathing solution: 150 NaCl, 2 KCl, 1.5 $CaCl_2$, 1 $MgCl_2$, 10 Hepes, (pH 7.4), 21–23°C. Na^+ currents in transfected cells for all clones ranged 2.5–15 nA. The maximal voltage error was < 5 mV. Leakage and capacitative currents were subtracted (-P/4 protocol). Currents were filtered at three and digitized at 20 kHz using pCLAMP (Axon Instruments). Data were analyzed using a combination of pCLAMP, EXCEL (Microsoft) and ORIGIN software (MicroCal). For statistic evaluation, Student's *t*-test was applied. Data are shown as means ± SEM.

Whole cell Na^+ currents for mutant and WT channels were elicited by voltage steps from a holding potential of −85 mV using 300 ms-prepulses to −120 mV. Representative raw current traces for all three clones are shown in Fig. 1A. The time course of FI was fit to a second order exponential function plus a constant term. The faster time constant, τ_h, accounted for > 95% of the current amplitude. There was a small but significant increase of τ_h for L1482A but not for L1482C channels in the range 0–52.5 mV (τ_h at 0 mV for WT, L1482C and L1482A, respectively: 0.42 ± 0.03 ms, 0.50 ± 0.03 ms and 0.79 ± 0.06 ms, $n = 14$, 13 and 8, $P < 0.000001$). The most obvious difference between both mutants and the WT was a considerable increase in persistent current, determined as the constant term of a second order exponential fit to 100 ms-test pulses, to 1.5 ± 0.3% (L1482C, $n = 13$) and 5.1 ± 0.9% (L1482A, $n = 8$) of peak current, compared to 0.2 ± 0.2% ($n = 14$) for the WT ($P < 0.001$). Using a pipette solution containing CsCl instead of CsF [10], the persistent current was 3.0 ± 0.5% (L1482C, $n = 7$) and 5.4 ± 0.6% (L1482A, $n = 10$) compared to 0.7 ± 0.3% (WT, $n = 7$) of peak current. Fluoride solutions were necessary to have long-lasting stable recordings for SI. Steady-state FI was slightly shifted in the depolarizing direction for L1482C but not L1482A channels and recovery from FI was accelerated for both clones (Fig. 1B,C). Thus, L1482A more than L1482C disrupt FI significantly. The shift in steady-state activation was not significant (Fig. 1B).

The data on FI for L1482A are in contrast to those previously reported by our group, where we could not find a significant difference between L1482A and WT channels [12]. The only plausible explanation we have for this discrepancy is a confusion of the mutant L1482A with another mutant or with WT in our previous study. We resequenced the two clones used now and did not find errors. We regret this mistake causing a conflict with data from McPhee and colleagues [11]. Now, our data are in line with their results, showing a significant persistent current for L1482A.

To determine the parameters of SI we first compared a conventional with a cumulative pulse protocol for steady-state SI (Fig. 2). Recovery from fast and slow inactivation after a 3-s conditioning pulse to 0 mV revealed that a 100-ms period at −100 mV is sufficient to let the channels recover from FI without occurrence of significant recovery from SI (Fig. 2A). Thus, all protocols to record SI contain a 100-ms recovery pulse to −100 mV before each test pulse. Cumulative protocols reduce measuring time considerably, since the long pulses for full recovery from SI are not used (Fig. 2B). Since there was almost no difference using the

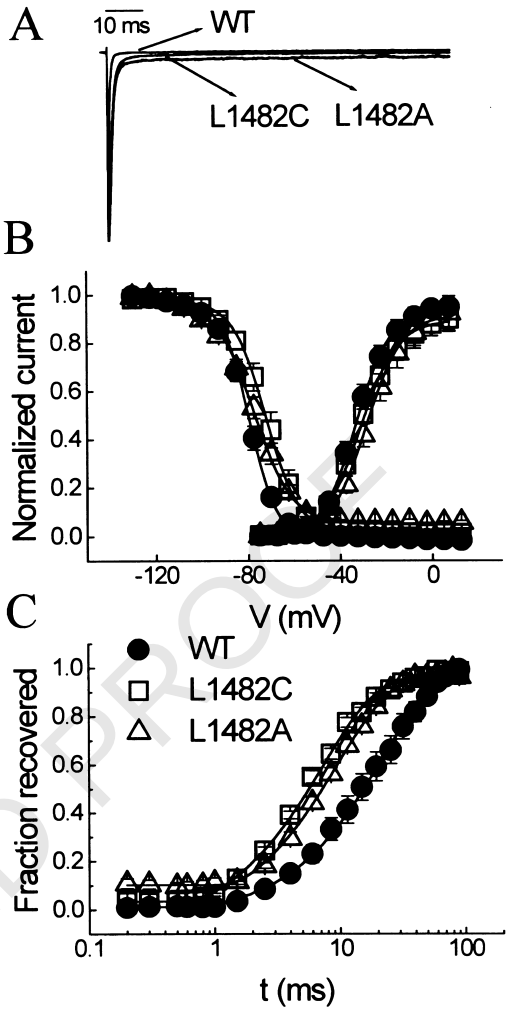

Fig. 1. Effects of mutations L1482C/A on FI. (A) Representative whole cell currents from cells transfected with cDNA of WT, L1482C or L1482A channels. (B) Voltage dependence of steady-state activation (right) and inactivation (left) for WT and mutant Na^+ channels. The conductance-voltage relationship for activation was obtained by 25 ms-depolarizing test pulses to the indicated potentials from a holding potential of −85 mV using 300 ms-prepulses to −120 mV. Lines are fits to a standard Boltzmann function: $G/G_{max} = 1/(1 + \exp[(V\text{-}V_{0.5})/k_V])$, with $V_{0.5}$ being the voltage of half-maximal activation and k_V a slope factor. Values for WT vs. L1482C and L1482A: $V_{0.5}$: −33.2 ± 1.7 vs. −31.4 ± 1.3 and −28.7 ± 1.6 mV; k_V: −6.7 ± 0.2 vs. −7.6 ± 0.3 and −7.3 ± 0.2 mV; $n = 10$, 13, 10, $P > 0.05$. Steady-state fast inactivation was determined using 300 ms-prepulses to the potentials indicated, followed by a short test pulse to −10 mV. Lines are fits to the Boltzmann function $I/I_{max} = 1/(1 + \exp[(V\text{-}V_{0.5})/k_V]) + C$. Values for WT vs. L1482C and L1482A: $V_{0.5}$: −79.7 ± 1.2 vs. −72 ± 2 ($P < 0.05$) and −77.7 ± 1.8 mV; k_V: 5.8 ± 0.2 vs. 7.2 ± 0.5 ($P < 0.001$) and 8.3 ± 0.3 mV ($P < 0.00001$); $n = 13$, 13, 10. (C) Recovery from FI at −80 mV after a 100-ms conditioning pulse to 0 mV. Lines are fits to a first order exponential function with time constants τ_{rec}=23 ± 4 vs. 7.3 ± 0.5 ($P < 0.005$) and 9.3 ± 0.6 ms ($P < 0.01$); $n = 4$, 5, 5 for WT vs. L1482C and L1482A.

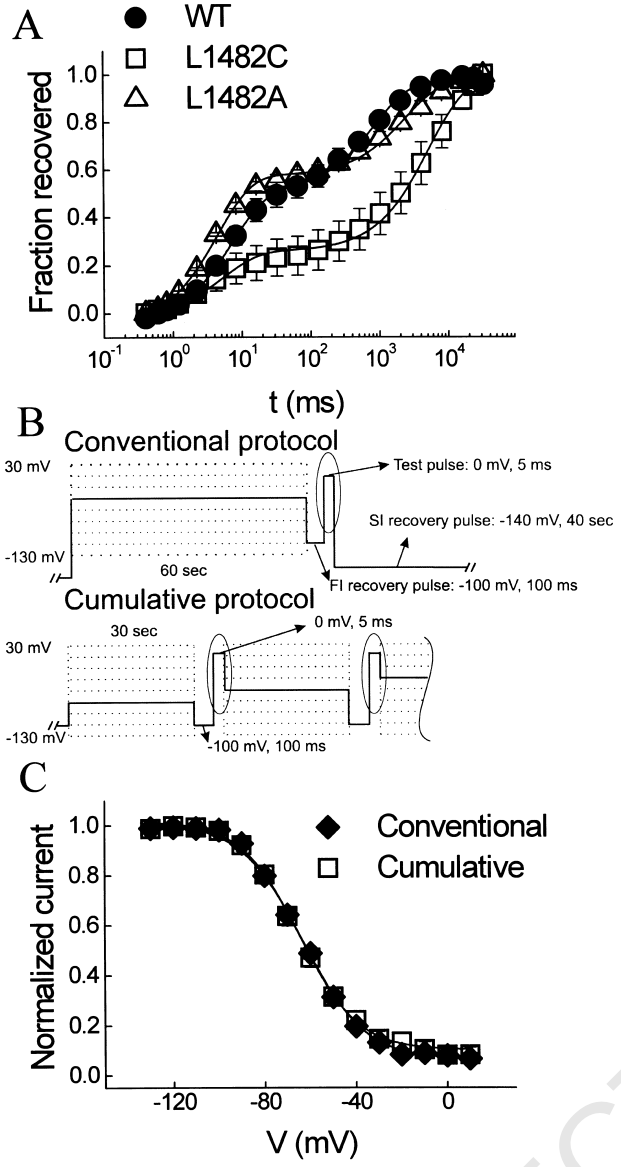

Fig. 2. Cumulative vs. conventional protocols for steady-state slow inactivation: (A) Time course of recovery from fast and slow inactivation after a 3 s-conditioning pulse to 0 mV. Lines are fits to a second order exponential function for fast and slow inactivation, respectively. (B) The two different pulse protocols used to measure steady-state slow inactivation. (C) Comparison between the alternative protocols reveals almost identical results. Lines are fits to a standard Boltzmann function with $V_{0.5}$: -62 ± 2 vs. -64 ± 3 mV; k_V: 13 ± 1 vs. 12 ± 1 mV; $n = 7, 6$ for the conventional and cumulative protocols, respectively.

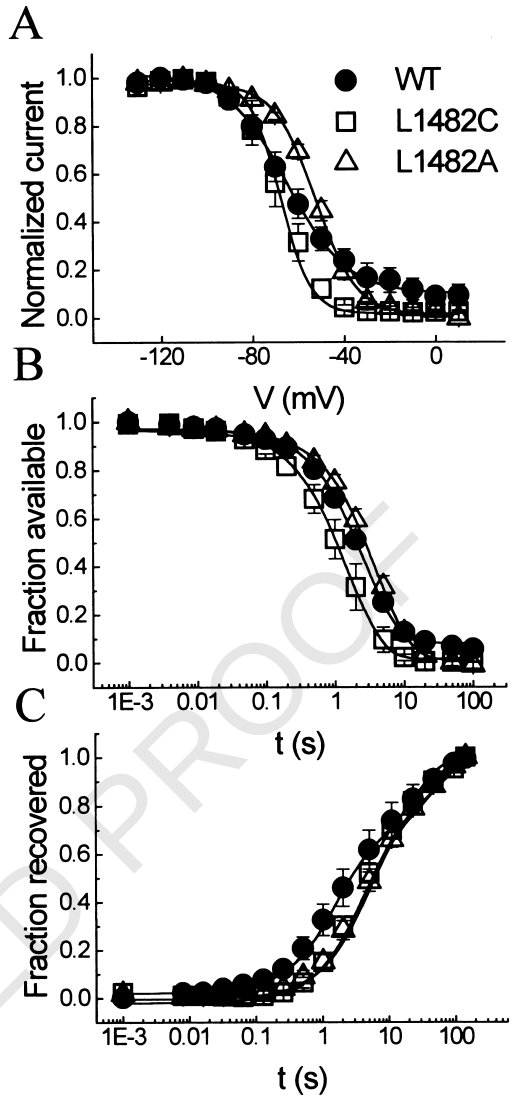

Fig. 3. Parameters of slow inactivation. (A) Steady state slow inactivation curve for WT, L1482C and L1482A channels, measured with the cumulative protocol. Data were fit to a Boltzmann function with values for WT vs. L1482C and L1482A: $V_{0.5}$: -64 ± 3 vs. -67 ± 3 and -53 ± 1 mV ($P < 0.01$); $k_{0.5}$: 12.2 ± 0.5 vs. 6.5 ± 0.4 ($P < 0.000001$) and 8.1 ± 0.3 mV ($P < 0.0001$); $n = 6$, 9, 7. (B) Entry into slow inactivation at 0 mV (cumulative protocol). Cells were held at -100 mV, depolarized to 0 mV for increasing duration as indicated on the abscissa, repolarized for 100 ms to -100 mV to let the channels recover from fast inactivation, and then depolarized again to -10 mV to determine the fraction of slow inactivated channels. The lines represent fits to a first order exponential function with the following time constants for WT vs. L1482C and L1482A: 2.8 ± 0.2 vs. 1.8 ± 0.5 and 4.4 ± 0.6 s ($P < 0.05$), $n = 8, 4, 6$ for WT vs. L1482C and L1482A. (C) Recovery from slow inactivation measured at -100 mV after a 30 s-conditioning pulse to 0 mV (cumulative protocol). Curves were best fit to a second order exponential function with the following time constants: $\tau_{srec1=}1.5 \pm 0.2$ vs. 4.7 ± 0.7 ($P < 0.005$) and 4.7 ± 0.8 s ($P < 0.05$); $\tau_{srec2=}22.9 \pm 5.7$ vs. 79 ± 36 and 54 ± 11 s; relative amplitude of $\tau_{srec1} = 57 \pm 6$ vs. 70 ± 2 and $66 \pm 2\%$, $n = 5$, 7, 9 for WT vs. L1482C and L1482A.

cumulative or conventional protocol (Fig. 2C), we used the cumulative protocol for comparison of mutant and WT channels.

Steady-state SI was significantly different for both mutations (Fig. 3A). The most obvious differences were a complete SI for the mutants, compared to $9 \pm 3\%$ (at 0 mV) of WT channels that did not enter the slow inactivated state, and a difference in slope of the availability curve. The midpoints of steady-state SI were shifted to the left for

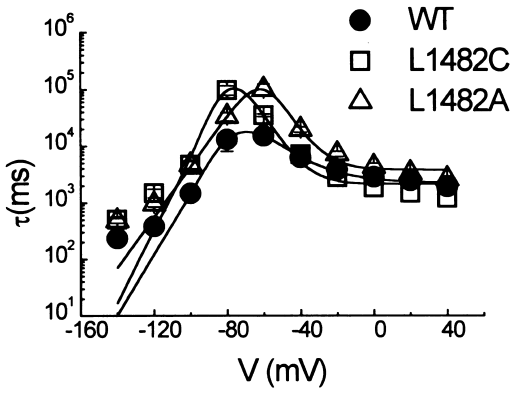

Fig. 4. Voltage dependence of time constants for entry (−60 to +40 mV) and recovery (−140 to −80 mV) of SI. The data are fit to a simple two-state kinetic model (slow inactivated, non-slow inactivated) with rate constants being exponential functions of voltage: on rate $\beta = \beta_0/(1 + \exp(-(V\text{-}V_{1/2})/k_\beta))$, off rate $\alpha = \alpha_0\exp(-V/k\alpha)$. We obtained the following parameters: WT: $\alpha_0 = 2.6 \times 10^{-6}s^{-1}$, $k_\alpha = 8.0$ mV, $\beta_0 = 0.44$ s^{-1}, $V_{1/2} = -29$ mV, $k_\beta = 16.8$ mV; L1482C: $\alpha_0 = 4.8 \times 10^{-8}s^{-1}$, $k_\alpha = 6.7$ mV, $\beta_0 = 0.46$ s^{-1}, $V_{1/2} = -36.9$ mV, $k_\beta = 8.4$ mV; L1482A: $\alpha_0 = 7.7 \times 10^{-6}s^{-1}$, $k_\alpha = 9.7$ mV, $\beta_0 = 0.26s^{-1}$, $V_{1/2} = -27.0$ mV, $k_\beta = 8.9$ mV.

L1482C and to the right for L1482A channels. Entry into and recovery from the slow inactivated state were also determined with cumulative protocols. The time course of entry was significantly accelerated for L1482C but not for L1482A (Fig. 3B and Fig. 4), whereas recovery from SI was significantly slowed for both mutations (Fig. 3C and Fig. 4). The voltage dependence of entry into and recovery from SI could be well fit using a two-state Eyring model with exponential functions of voltage for entry and recovery (Fig. 4). The discrepancy of the fit with the experimental data at potentials more negative than −100 mV can be explained by the second order exponential function required to describe the time course of recovery from SI.

Our results show a significant role of the C-terminal end of the IV/S4-S5 loop for SI of the voltage-gated Na^+ channel. Whereas a conclusive hypothesis can be formulated as to how this structure is involved in FI (see beginning and Refs.[7,10–12]) it is difficult even to speculate upon a mechanism as to how the IV/S4-S5 loop contributes to SI. Most problematic is the absence of a valuated model detailing how SI functions in general. Several regions like the pore [2], the voltage sensors [1,13,15], S4-S5 loops [5,8], S5 [3] and S6 [8] segments are important for regular function of SI. Complementary to these previous results, our data suggest that upon depolarization a slow structural rearrangement occurs in the region involving S4, S4-S5 and S5 segments in domain IV contributing significantly to the formation of the slow inactivated state. Whereas L1482A had stronger effects on disruption of FI, L1482C enhanced SI more extensively. Hence in summary, there seem to be fast and slow conformational changes in this protein region influencing the different states of inactivation in distinct ways.

This work was supported by the Deutsche Forschungsgemeinschaft (DFG Le1030/5–1).

[1] Alekov, A., Rahman, M.M., Mitrovic, N., Lehmann-Horn, F. and Lerche, H., A Na^+ channel mutation causing epilepsy in man exhibits subtle defects in fast inactivation and activation in vitro, J. Physiol., 529 (2000) 533–539.
[2] Balser, J.R., Nuss, H.B., Chiamvimonvat, N., Perez Garcia, M.T., Marban, E. and Tomaselli, G.F., External pore residue mediates slow inactivation in mu 1 rat skeletal muscle Na^+ channels, J. Physiol., 494 (1996) 431–442.
[3] Bendahhou, S., Cummins, T.R., Tawil, R., Waxman, S.G. and Ptacek, L.J., Activation and inactivation of the voltage-gated Na^+ channel: role of segment S5 revealed by a novel hyperkalaemic periodic paralysis mutation, J. Neurosci., 19 (1999) 4762–4771.
[4] Catterall, W.A., From ionic currents to molecular mechanisms: the structure and function of voltage-gated Na^+ channels, Neuron, 26 (2000) 13–25.
[5] Cummins, T.R. and Sigworth, F.J., Impaired slow inactivation in mutant Na^+ channels, Biophys. J., 71 (1996) 227–236.
[6] Featherstone, D.E., Richmond, J.E. and Ruben, P.C., Interaction between fast and slow inactivation in Skm1 Na^+ channels, Biophys. J., 71 (1996) 3098–3109.
[7] Filatov, G.N., Nguyen, T.P., Kraner, S.D. and Barchi, R.L., Inactivation and secondary structure in the D4/S4–5 region of the SkM1 Na^+ channel, J. Gen. Physiol., 111 (1998) 703–715.
[8] Hayward, L.J., Brown Jr, R.H. and Cannon, S.C., Slow inactivation differs among mutant Na channels associated with myotonia and periodic paralysis, Biophys. J., 72 (1997) 1204–1219.
[9] Lehmann-Horn, F. and Jurkat-Rott, K., Voltage-gated ion channels and hereditary disease, Physiol. Rev., 79 (1999) 1317–1372.
[10] Lerche, H., Peter, W., Fleischhauer, R., Pika-Hartlaub, U., Malina, T., Mitrovic, N. and Lehmann-Horn, F., Role in fast inactivation of the IV/S4-S5 loop of the human muscle Na^+ channel probed by cysteine mutagenesis, J. Physiol., 505 (1997) 345–352.
[11] McPhee, J.C., Ragsdale, D.S., Scheuer, T. and Catterall, W.A., A critical role for the S4-S5 intracellular loop in domain IV of the Na^+ channel alpha-subunit in fast inactivation, J. Biol. Chem., 273 (1998) 1121–1129.
[12] Mitrovic, N., Lerche, H., Heine, R., Fleischhauer, R., Pika-Hartlaub, U., Hartlaub, U., George, A.L. and Lehmann-Horn, F., Role in fast inactivation of conserved amino acids in the IV/S4-S5 loop of the human muscle Na^+ channel, Neurosci. Lett., 214 (1996) 9–12.
[13] Mitrovic, N., George Jr, A.L. and Horn, R., Role of domain 4 in Na^+ channel slow inactivation, J. Gen. Physiol., 115 (2000) 707–718.
[14] Nuss, H.B., Balser, J.R., Orias, D.W., Lawrence, J.H., Tomaselli, G.F. and Marban, E., Coupling between fast and slow inactivation revealed by analysis of a point mutation (F1304Q) in μ1 rat skeletal muscle Na^+ channels, J. Physiol., 494 (1996) 411–429.
[15] Struyk, A.F., Scoggan, K.A., Bulman, D.E. and Cannon, S.C., The human skeletal muscle Na^+ channel mutation R669H associated with hypokalemic periodic paralysis enhances slow inactivation, J. Neurosci., 20 (2000) 8610–8617.
[16] Vedantham, V. and Cannon, S.C., Slow inactivation does not affect movement of the fast inactivation gate in voltage-gated Na^+ channels, J. Gen. Physiol., 111 (1998) 83–93.